Applied Mathematics E-Notes, 22(2022), 146-158 © ISSN 1607-2510
Available free at mirror sites of http://www.math.nthu.edu.tw/∼amen/

Numerical Solution Of Fractional Model Of Atangana-Baleanu-Caputo Integrodifferential Equations With Integral Boundary Conditions*

Mohammad Alneimat†, Maher Moakher‡, Nadir Djeddi§, Shrideh Al-Omari¶

Received 18 February 2022

Abstract

In this analysis, we propose an advanced numerical technique, reproducing kernel discretization method (RKDM), to investigate numerical solutions for a class of systems of fractional integro-differential equations (SFIDE) with integral boundary conditions. The Atangana-Baleanu fractional derivative is used to formulate the fractional integro-differential equations. The solution methodology is mainly based on constructing a reproducing kernel function, that satisfies the integral boundary conditions, in order to construct an orthonormal basis to formulate the solution in form of Fourier series that is uniformly convergent in the specified space $W_2^2[a,b]$. Numerical applications are investigated to represent the hypothesis and to confirm the design steps of the proposed advanced technique. The numerical viewpoint indicates that the RKDM is an important tool for dealing with such issues arising in physics and engineering fields.

1 Introduction

Fractional integro-differential equations are combinations of differential and integral differential equations with arbitrary order. These equations often arise in the mathematical modeling of complex systems and problems in many branches of engineering and applied mathematics such as fluid dynamics, electromagnetic, electrodynamics, chemical kinetics, elasticity, biomechanics, biological models, and oscillation theory [1, 2, 3, 4, 5]. Nowadays, the fractional integro-differential equations with integral boundary conditions constitute a very significant and important class of problems; that integral boundary condition came up when the values of the required solution at boundary were connected to the values of interior points of the domain [6, 7, 8, 9]. The choice of the type of fractional derivative operator implemented during the mathematical formulation of systems controls the determination of the eligibility and efficiency of the study embodied in these systems, because it provides high-quality and excellent tools that contribute to decoding complex structures without compromising the genetic properties of systems. There are many different kinds of fractional derivatives operators. All of them include integral operators with different regularity properties and some have both singular and non-singular kernels [10]. At any rate, among the more renowned definitions that are commonly circulated in research papers, we mention Riemann-Liouville's and Caputo's fractional definitions. Despite their frequent use as a result of their close association with the beginning of laying the foundations of fractional calculus, these fractional operators suffer from some shortcomings, especially when it comes to having singular kernels, which puts us a lot of question marks about knowing the behavior and history of the phenomenon at that point.

*Mathematics Subject Classifications: 20F05, 20F10, 20F55, 68Q42.

†Laboratory for Mathematical and Numerical Modeling in Engineering Science, National Engineering School at Tunis, University of Tunis El Manar, Tunis-Belvédère, Tunisia

‡Laboratory for Mathematical and Numerical Modeling in Engineering Science, National Engineering School at Tunis, University of Tunis El Manar, Tunis-Belvédère, Tunisia

§Department of Mathematics and Computer Science, Larbi Tebessi University, Tebessa, 12002, Algeria Nonlinear Dynamics Research Center (NDRC), Ajman University, Ajman, UAE

¶Department of Scientific Basic Sciences, Faculty of Engineering Technology, Al-Balqa Applied University, Amman 11134, Jordan

Recently, as part of the strenuous efforts made by researchers to update and improve the performance of fractional operators in order to avoid the sterility that may fall into them, Atangana and Baleanu suggested a novel fractional operator in the Caputo sense based primarily on the generalized Mittag-Leffler function [11, 12]. This operator has the advantage of possessing a non-singular and non-local kernel, which enables us to describe complex systems that follow at the same time the law of power and exponential decay in a unique way and with great efficiency compared to other available fractional operators.

In this work, we consider the following system of fractional integro-differential equations

$$ {}_{a}^{ABC}\mathfrak{D}_{x}^{\alpha_s} u_s(x) = f_s(x) + \sum_{l=1}^{2} \int_a^x H_{s,l}(x,\tau) u_l(\tau) d\tau, \ \ s = 1, 2, \tag{1} $$

with integral boundary conditions

$$ u_s(a) + \eta_s u_s(b) + \lambda_s \int_a^b p_s(\tau) u_s(\tau) d\tau = 0 \tag{2} $$

where η_s and λ_s, $(s = 1, 2)$ are real constants; f_s, p_s, and $H_{s,k}$, $(k = 1, 2,\ s = 1, 2)$ are continuous functions; u_s, $(s = 1.2)$ are the unknown functions to be determined. Here, ${}_{a}^{ABC}\mathfrak{D}_{x}^{\alpha_s}$ denotes the Atangana-Baleanu fractional derivative of order α_s such that $\alpha_s \in [0, 1)$.

Due to the importance of these systems in various engineering and applied fields, as well as the difficulty of finding closed solutions to them due to the inability of traditional methods to deal with the complexities of non-linear formulation of systems, as well as the complexities of the implemented fractional operator. In this work, we aim to employ an advanced numerical method based on reproducing kernel theory, in order to explore the numerical and analytic solutions of this class of SFIDEs with integral boundary conditions. The concept of reproducing kernels theory was first introduced by Zaremba in his research paper [13] to be followed by more related papers that established the birth of an advanced and integrated iterative method. The reproducing kernel theory has played significant role in many successful applications in numerical analysis, differential equation, fuzzy differential equations, difference equations, probability and statistics and so on, see [14]–[31] and [33].

This paper is arranged as follows: In section 2, some elementary definitions and concepts of the fractional operator used are presented. In section 3, the reproducing kernel Hilbert space associated with SFIDE (1) is investigated. In section 4, our fundamental results are presented. In section 5, some test examples and computational results are obtained. Finally, some concluding remarks are presented in the end.

2 The Atangana-Baleanu Fractional Derivative

In this section, we introduce the elementary definitions of the novel fractional derivatives proposed by Atangana and Baleanu [11].

Definition 1 *The Mittag-Leffler function $E_\alpha(x)$ is defined as*

$$ E_\alpha(x) = \sum_{k=0}^{\infty} \frac{x^k}{\Gamma(\alpha k + 1)}, \quad \alpha > 0. $$

This function provides the simplest nontrivial generalization of the exponential function in which the factor $k! = \Gamma(k + 1)$ is replaced by $(\alpha k)! = \Gamma(\alpha k + 1)$.

Definition 2 *The Sobolev space $H^1[a, b]$ is defined as follow:*

$$ H^1[a, b] = \{v \mid v^{(j)} \text{ is Abs. Cont.}, \ j = 1, 2, \ldots, m-1, \ v^{(m)} \in L^2([a, b])\}. $$

Definition 3 *The Atangana-Baleanu fractional derivative in Caputo sense is presented as*

$$ {}^{ABC}_{a}\mathfrak{D}^{\alpha}_{x}u(x) = \frac{B(\alpha)}{1-\alpha}\int_{a}^{x} u'(\tau)E_{\alpha}\left(-\frac{\alpha}{1-\alpha}(x-\tau)^{\alpha}\right)d\tau, \tag{3} $$

for $0 \leq \alpha \leq 1$, $a \leq x \leq b$, *and* $u(x) \in H^1[a,b]$.

Definition 4 *The Atangana-Baleanu fractional derivative in Riemann-Liouville sense is presented as*

$$ {}^{ABR}_{a}\mathfrak{D}^{\alpha}_{x}u(x) = \frac{B(\alpha)}{1-\alpha}\frac{d}{dx}\int_{a}^{x} u(\tau)E_{\alpha}\left(-\frac{\alpha}{1-\alpha}(x-\tau)^{\alpha}\right)d\tau, \tag{4} $$

for $0 \leq \alpha \leq 1$, $a \leq x \leq b$, *and* $u(x) \in H^1[a,b]$ *which may not be differentiable.*

In the above definitions, $B(\alpha)$ is the normalization function which depends on α and satisfies $B(\alpha) = 1-\alpha+\frac{\alpha}{\Gamma(\alpha)}$ such that $B(0) = B(1) = 1$.

Definition 5 *The fractional integral associated to the Atangana-Baleanu fractional derivative is defined as*

$$ {}^{AB}_{a}\mathfrak{I}^{\alpha}_{x}u(x) = \frac{1-\alpha}{B(\alpha)}u(x) + \frac{\alpha}{B(\alpha)\Gamma(\alpha)}\int_{a}^{x} u(\tau)(x-\tau)^{\alpha-1}d\tau. \tag{5} $$

3 Reproducing Kernel Hilbert Space

In this section, we construct the reproducing kernel Hilbert space associated with SFIDE (1)–(2).

Definition 6 *Suppose that* $(H, \|\cdot\|_H)$ *is a Hilbert space of real functions defined on an abstract set* Ω. *A function* $K : \Omega \times \Omega \longrightarrow \mathbb{R}$ *that satisfies the following two conditions*

(a) $K_x(\cdot) = K(\cdot, x) \in H$, $\forall x \in \Omega$;

(b) $\langle f(\cdot), K(\cdot, x)\rangle_H = f(x)$, $\forall x \in \Omega$ *and* $\forall f \in H$,

is called a reproducing kernel function for H.

The last condition is knows as "the reproducing property", which reproduces the value of the function $f(\cdot)$ at the point x by the inner product of $f(\cdot)$ with $K_x(\cdot)$.

We will indicate to such Hilbert space H that has a reproducing kernel function as a reproducing kernel Hilbert space.

Now, in a way similar to what Geng and Cui did in [14], we construct the reproducing kernel Hilbert space $W_2^2[a,b]$.

Definition 7 *The space* $W_2^2[a,b]$ *is defined as follows:*

$$ \begin{aligned} W_2^2[a,b] \quad = \quad & \Big\{u(x) : u,\ u' \text{ are univariate absolutely continuous real-valued functions,} \\ & u^{(2)} \in L^2[a,b],\ u(a) + \eta u(b) + \lambda\int_a^b p(\tau)u(\tau)d\tau = 0\Big\}. \end{aligned} $$

The inner product and norm associated with $W_2^2[a,b]$ *are given, respectively, by*

$$ \langle u(x), v(x)\rangle_{W_2^2} = \sum_{i=0}^{1} u^{(i)}(a)v^{(i)}(a) + \int_a^b u^{(2)}(x)v^{(2)}(x)dx, \tag{6} $$

and $\|u\|^2_{W_2^2} = \langle u(x), u(x)\rangle_{W_2^2}$, *where* $u,\ v \in W_2^2[a,b]$.

Theorem 1 *The space $W_2^2[a,b]$ is a complete reproducing kernel Hilbert space and the unique representation of reproducing kernel function $K_x(\tau)$ of $W_2^2[a,b]$ can be obtained as follows:*

$$K_x(\tau) = \begin{cases} \sum_{k=1}^{4} a_k(x)\tau^{k-1} - cH(y), & \tau < x, \\ \sum_{k=1}^{4} b_k(x)\tau^{k-1} - cH(y), & x \le \tau, \end{cases} \tag{7}$$

where $H(y) = \int_a^{\tau}\int_a^{\tau_4}\int_a^{\tau_3}\int_a^{\tau_2} h(\tau_1)\, d\tau_1\, d\tau_2\, d\tau_3\, d\tau_4$.

Proof. From Eq. (6), we have

$$\begin{aligned} \langle u(\tau), K_x(\tau)\rangle_{W_2^2} &= \sum_{i=0}^{1} u^{(i)}(a)K_x^{(i)}(a) + \int_a^b u^{(2)}(\tau)K_x^{(2)}(\tau)dx \\ &\quad + c\left[u(a) + \eta u(b) + \lambda\int_a^b p(\tau)u(\tau)d\tau\right]. \end{aligned} \tag{8}$$

By successive integration by parts for Eq. (8), it becomes

$$\begin{aligned} \langle u(\tau), K_x(\tau)\rangle_{W_2^2} &= u(a)\left[K_x(a) + K_x^{(3)}(a) + c\right] + u'(a)\left[K_x^{(1)}(a) - K_x^{(2)}(a)\right] \\ &\quad - u(b)\left[K_x^{(3)}(b) + c\eta\right] + u'(b)K_x^{(2)}(b) + \int_a^b u(\tau)\left[K_x^{(4)}(\tau) - ch(\tau)\right]d\tau. \end{aligned} \tag{9}$$

Since $K_x(\tau) \in W_2^2[a,b]$, $K_x(\tau)$ satisfies

$$K_x(a) + \eta K_x(b) + \lambda\int_a^b p(\tau)K_x(\tau)d\tau = 0. \tag{10}$$

If

$$K_x(a) + K_x^{(3)}(a) + c = 0, \quad K_x^{(1)}(a) - K_x^{(2)}(a) = 0, \tag{11}$$

$$K_x^{(3)}(b) + c\eta = 0 \ \text{ and } \ K_x^{(2)}(b) = 0, \tag{12}$$

then

$$\langle u(\tau), K_x(\tau)\rangle_{W_2^2} = \int_a^b u(\tau)\left[K_x^{(4)}(\tau) - ch(\tau)\right]d\tau. \tag{13}$$

Now, with the aid of reproducing kernel property, we can get

$$K_x^{(4)}(\tau) - ch(\tau) = \delta(\tau - x). \tag{14}$$

The corresponding characteristic equation of Eq. (14) is given by

$$r^4 = 0. \tag{15}$$

Consequently, we can obtain characteristic values $r = 0$ whose multiplicity is 4. Then, let

$$K_x(\tau) = \begin{cases} \sum_{k=1}^{4} a_k(x)\tau^{k-1} - cH(y), & \tau < x, \\ \sum_{k=1}^{4} b_k(x)\tau^{k-1} - cH(y), & x \le \tau, \end{cases}$$

where, $H(y) = \int_a^{\tau}\int_a^{z}\int_a^{t}\int_a^{s} h(r)\, dr\, ds\, dt\, dz$.

On the other hand, the unknown coefficients $a_k(x)$ and $b_k(x)$ are determined by

$$K_x^{(k)}(x+0) = K_x^{(k)}(x-0), \quad k = 1,2,3. \tag{16}$$

Also,

$$K_x^{(4)}(x+0) - K_x^{(4)}(x-0) = 1. \tag{17}$$

From (10)–(12), (16), and (17), the unknown coefficients of Eq. (7) can be determined. ■

In [14], Li and Cui determine the reproducing kernel Hilbert space $W_2^1[a,b]$ as follows:

$$W_2^1[a,b] = \{u(x) : u \text{ is one variable absolutely continuous real-valued function, } u' \in L^2[a,b]\}.$$

The inner product and norm associated with $W_2^1[a,b]$ are given, respectively, by

$$\langle u(x), v(x)\rangle_{W_2^1} = \int_a^b \left(u(x)v(x) + u'(x)v'(x)\right) dx, \tag{18}$$

and $\|u\|^2_{W_2^1} = \langle u(x), u(x)\rangle_{W_2^1}$, where $u,\, v \in W_2^1[a,b]$.

Also, its reproducing kernel function as follows:

$$\bar{K}_x(\tau) = \frac{1}{\sinh(1)}\left[\cosh(x+\tau-1) + \cosh(|x-\tau|-1)\right].$$

4 Description of the Method

In this section, we explain the practical steps of the RKDM proposed for solving the system (1)–(2). We first define a linear differential operator as follows

$$L_s : W_2^2[a,b] \longrightarrow W_2^1[a,b], \quad a \le x \le b, \tag{19}$$

such that

$$L_s u(x) = {}_a^{ABR}\mathfrak{D}_x^{\alpha_s} u_s(x); \quad s = 1, 2.$$

Then the system (1)–(2) can be converted into

$$L_s u(x) = f_s(x) + \sum_{l=1}^{2} \int_a^x H_{s,l}(x,\tau) u_l(\tau) d\tau, \quad s = 1, 2, \tag{20}$$

with integral boundary conditions

$$u_s(a) + \eta_s u_s(b) + \lambda_s \int_a^b p_s(\tau) u_s(\tau) d\tau = 0. \tag{21}$$

Here, it is clear that $L_s : W_2^2[a,b] \longrightarrow W_2^1[a,b]$; $s = 1, 2$ is a linear and bounded operator. In the following we construct an orthogonal function system of $W_2^2[a,b]$ as follows: Choose a countable dense subset $\{x\}_{i=0}^{\infty}$ in $[a,b]$, put $\Phi_i^{\{s\}}(x) = \bar{K}_{x_i}(x)$ and $\Psi_i^{\{s\}}(x) = L_s^{\star}\Phi_i^{\{s\}}(x)$, where $L_s^{\star}$ is the conjugate operator of L and $s = 1, 2$. The orthonormal function systems $\{\widehat{\Psi}_i^{\{s\}}(x)\}_{i=0}^{\infty}$ of $W_2^2[a,b]$ can be constructed by applying Gram-Schmidt orthogonalization process of $\{\Psi_i^{\{s\}}(x)\}_{i=0}^{\infty}$ as follows:

$$\widehat{\Psi}_i^{\{s\}}(x) = \sum_{k=1}^{i} \gamma_{ik}^{\{s\}} \Psi_i^{\{s\}}(x); \quad i = 1, 2, \ldots, \; s = 1, 2,$$

where, $\gamma_{ik}^{\{s\}}$ are the orthogonalization coefficients such that $\gamma_{ii}^{\{s\}} > 0$, and are obtained using the following algorithm:

Algorithm 1 The steps of Gram–Schmidt orthogonalization process

procedure : DO THE NEXT STEPS TO OBTAIN $\{\widehat{\Psi}_i^{\{s\}}(x)\}_{i=1}^{\infty}$ OF $W_2^2[a,b]$.

Step I:

for $i = 1$ to n and $k = 1$ to i **do**

$$\gamma_{ik}^{\{s\}}\,|_{i=k=1} = \frac{1}{\|\Psi_i^{\{s\}}(x)\|_{W_2^2}},$$

$$\gamma_{ik}^{\{s\}}\,|_{i=k\neq 1} = \frac{1}{\sqrt{\|\Psi_i^{\{s\}}(x)\|_{W_2^2}^2 - \sum_{p=1}^{i-1}\langle \Psi_i^{\{s\}}(x), \widehat{\Psi}_p^{\{s\}}(x)\rangle_{W_2^2}}},$$

$$\gamma_{ik}^{\{s\}}\,|_{i>k} = -\frac{1}{\sqrt{\|\Psi_i^{\{s\}}(x)\|_{W_2^2}^2 - \sum_{p=1}^{i-1}\langle \Psi_i^{\{s\}}(x), \widehat{\Psi}_p^{\{s\}}(x)\rangle_{W_2^2}^2}} \sum_{p=k}^{i-1}\langle \Psi_i^{\{s\}}(x), \widehat{\Psi}_p^{\{s\}}(x)\rangle_{W_2^2}\gamma_{pk}^{\{s\}},$$

Step II:

for $i = 1$ to n **do**

$$\widehat{\Psi}_i^{\{s\}}(x) = \sum_{k=1}^{i}\gamma_{ik}^{\{s\}}\Psi_i^{\{s\}}(x).$$

Theorem 2 *If $\{x_i\}_{i=1}^{\infty}$ is a dense subset on $[a,b]$, then $\{\Psi_i^{\{s\}}(x)\}_{i=1}^{\infty}$ is a complete function system in $W_2^2[a,b]$ with $\Psi_i^{\{s\}}(x) = (L_s)_\tau K_x(\tau)\,|_{\tau=x_i}$ such that $(L_s)_\tau$ indicates that the operator L_s, $s = 1,2$ is applied to the function of τ.*

Proof. Note here that

$$\begin{aligned}\Psi_i^{\{s\}}(x) &= L_s^\star\Phi_i^{\{s\}}(\tau) = \langle L_s^\star\Phi_i^{\{s\}}(\tau), K_x(\tau)\rangle_{W_2^2}\\ &= \langle \Phi_i^{\{s\}}(\tau), L_sK_x(\tau)\rangle_{W_2^1} = (L_s)_\tau K_x(\tau)\,|_{\tau=x_i}.\end{aligned}$$

Now, look at the completeness of the sequence $\{\Psi_i^{\{s\}}(x)\}_{i=1}^{\infty}$ in $W_2^2[a,b]$. For each fixed $u_s(x) \in W_2^2[a,b]$, let $\langle u_s(x), \Psi_i^{\{s\}}(x)\rangle_{W_2^2} = 0$, $i = 1,2,\ldots$, so that

$$\langle u_s(x), \Psi_i^{\{s\}}(x)\rangle_{W_2^2} = \langle u_s(x), L_s^\star\Phi_i^{\{s\}}(x)\rangle_{W_2^2} = \langle L_su_s(x), \Phi_i^{\{s\}}(x)\rangle_{W_2^2} = L_su_s(x_i) = 0.$$

Since $\{x_i\}_{i=1}^{\infty}$ is a dense subset on $[a,b]$ and L_s^{-1} exist, we obtain $u_s(x) = 0$ for $s = 1,2$. ■

Now, we give the representation expression of analytical and approximate solutions of system (20)–(21).

Theorem 3 *If $\{x_i\}_{i=1}^{\infty}$ is a dense subset on $[a,b]$ and the solution of SFIDE (20)–(21) is unique and L_s^{-1} exists then a formula of the solution can be expressed as follows:*

$$u_s(x) = \sum_{i=1}^{\infty} A_i^{\{s\}}\widehat{\Psi}_i^{\{s\}}(x), \tag{22}$$

where, $A_i^{\{s\}} = \sum_{k=1}^{i}\gamma_{ik}^{\{s\}}\left(f_s(x_k) + \sum_{l=1}^{2}\int_a^{x_k} H_{s,l}(x_k,\tau)u_l(\tau)d\tau\right)$ such that $\gamma_{ik}^{\{s\}}$ are the orthogonalization coefficients and $s = 1,2$.

Proof. Using the previous theorem, it is easy to show that $\{\widehat{\Psi}_i^{\{s\}}(x)\}_{i=1}^{\infty}$ is the complete orthonormal basis of $W_2^2[a,b]$. Note that, $\langle u_s(x), \Phi_i^{\{s\}}(x)\rangle_{W_2^1}$, for each $u_s(x) \in W_2^1[a,b]$. Hence, we have

$$\begin{aligned}u_s(x) &= \sum_{i=1}^{\infty}\langle u_s(x), \widehat{\Psi}_i^{\{s\}}(x)\rangle_{W_2^2}\widehat{\Psi}_i^{\{s\}}(x)\\ &= \sum_{i=1}^{\infty}\sum_{k=1}^{i}\gamma_{ik}^{\{s\}}\langle u_s(x), \Psi_i^{\{s\}}(x)\rangle_{W_2^2}\widehat{\Psi}_i^{\{s\}}(x)\end{aligned}$$

$$
\begin{aligned}
&= \sum_{i=1}^{\infty}\sum_{k=1}^{i}\gamma_{ik}^{\{s\}}\langle u_s(x), L^{\star}\Phi_k^{\{s\}}(x)\rangle_{W_2^2}\widehat{\Psi}_i^{\{s\}}(x)\\
&= \sum_{i=1}^{\infty}\sum_{k=1}^{i}\gamma_{ik}^{\{s\}}\langle L_s u_s(x), \Phi_k^{\{s\}}(x)\rangle_{W_2^1}\widehat{\Psi}_i^{\{s\}}(x)\\
&= \sum_{i=1}^{\infty}\sum_{k=1}^{i}\gamma_{ik}^{\{s\}}\left(f_s(x_k)+\sum_{l=1}^{2}\int_a^{x_k}H_{s,l}(x_k,\tau)u_l(\tau)d\tau\right)\widehat{\Psi}_i^{\{s\}}(x)\\
&= \sum_{i=1}^{\infty}A_i^{\{s\}}\widehat{\Psi}_i^{\{s\}}(x).
\end{aligned}
$$

■

The approximate solution $u_{s,n}(x)$ can be obtained by taking finitely many terms in the series representation of $u_s(x)$ and

$$u_{s,n}(x)=\sum_{i=1}^{n}A_i^{\{s\}}\widehat{\Psi}_i^{\{s\}}(x). \tag{23}$$

Lemma 1 *If $u_s(x)\in W_2^2[a,b]$, then there exists positive real number c_s such that*

$$|u_s^{(i)}(x)|\le c_s\|u(x)\|_{W_2^2},\quad i=0,1,\ \text{and } s=1,2.$$

Theorem 4 *Suppose that $u_s(x)$ is the unique solution of SFIDE (1)–(2) and $\varepsilon_{s,n}$ is the error between the exact $u_s(x)$ and the approximate $u_{s,n}(x)$ for $s=1,2$. Then, the norm $\|\cdot\|_{W_2^2}$ of the error $\varepsilon_{s,n}$ is monotone decreasing.*

Proof. From the formula (22) and (23), it yields that

$$
\begin{aligned}
\|\varepsilon_{s,n}\|_{W_2^2}^2 &= \left(\sum_{i=n+1}^{\infty}\sum_{k=1}^{i}\gamma_{ik}^{\{s\}}\left(f_s(x_k)+\sum_{l=1}^{2}\int_a^{x_k}H_{s,l}(x_k,\tau)u_l(\tau)d\tau\right)\widehat{\Psi}_i^{\{s\}}(x)\right)\\
&= \sum_{i=n+1}^{\infty}\left(\sum_{k=1}^{i}\gamma_{ik}^{\{s\}}\left(f_s(x_k)+\sum_{l=1}^{2}\int_a^{x_k}H_{s,l}(x_k,\tau)u_l(\tau)d\tau\right)\right)^2.
\end{aligned}\tag{24}
$$

The above formula shows that the square norm of the error $\varepsilon_{s,n}$ is monotone decreasing, and the proof is complete. ■

5 Computation experiments

In this section, we consider some meaningful numerical examples in order to illustrate the efficiency and reliability of the proposed method for solving the SFIDE (1)–(2). All symbolic and numerical results were performed by using the MATHEMATICA 12 software package.

Example 1 *Consider the following SFIDE*

$$
\begin{cases}
{}_0^{ABC}\mathfrak{D}_x^{\alpha}u_1(x)=\int_0^x(x-\tau)(u_1(\tau)+u_2(\tau))\,d\tau-\sin(x)+\cos(x)-2,\\
{}_0^{ABC}\mathfrak{D}_x^{\alpha}u_2(x)=\int_0^x(x-\tau)(u_1(\tau)-u_2(\tau))\,d\tau-\sin(x)-2(\sin(x)-x)+\cos(x),
\end{cases}
$$

subject to the integral boundary conditions:

$$
\begin{cases}
u_1(0)+\frac{1}{2\sin(1)-1}u_1(1)-\int_0^1\frac{1}{2\sin(1)-1}u_1(x)dx=0,\\
u_2(0)+\frac{1}{1-2\cos(1)}u_2(1)-\int_0^1\frac{1}{1-2\cos(1)}u_2(x)dx=0,
\end{cases}
$$

where, $0 \leq \alpha \leq 1$. *The exact solution at* $\alpha = 1$ *is*

$$\begin{cases} u_1(x) = \cos(x) - \sin(x), \\ u_2(x) = \cos(x) + \sin(x). \end{cases}$$

Indeed, the exact solution at the fractional value of α *is not available.*

By applying the proposed method to solve Example (1). We display the numerically representative results in Tables 1–4. Error analysis at some selected grid points with step size $h = 0.16$ *and* $n = 51$ *when* $\alpha = 1$ *are summarized in Tables 1 and 2. Furthermore, using the present method, we pick uniform grid points* $x_k = \frac{k-1}{n-1}$, $i = 1, 2, \ldots, n$. *The numerical outcomes for different values of the fractional-order* α *are given in Tables 3 and 4 to explain the approximate solutions such that* $\alpha \in \{0.75, 0.85, 0.95, 1\}$ *and* $n = 21$.

Table 1: Numerical outcomes for the solution $u_1(x)$ of Example (1) at $\alpha = 1$.

x_k	$u_1(x_k)$	$u_{1,51}(x_k)$	$\lvert u_1(x_k) - u_{1,51}(x_k)\rvert$	$\left\lvert\frac{u_1(x_k)-u_{1,51}(x_k)}{u_1(x_k)}\right\rvert$
0.16	0.827909	0.827916	7.0817×10^{-6}	8.55372×10^{-6}
0.32	0.634669	0.634680	1.1569×10^{-5}	1.82297×10^{-5}
0.48	0.425216	0.425229	1.3612×10^{-5}	3.20122×10^{-5}
0.64	0.204900	0.204912	1.1476×10^{-5}	5.60098×10^{-5}
0.80	-0.0206494	-0.020645	3.4331×10^{-6}	1.66259×10^{-4}
0.96	-0.2456720	-0.245684	1.2223×10^{-5}	4.97537×10^{-5}

Table 2: Numerical outcomes for the solution $u_2(x)$ of Example (1) at $\alpha = 1$.

x_k	$u_2(x_k)$	$u_{2,51}(x_k)$	$\lvert u_2(x_k) - u_{2,51}(x_k)\rvert$	$\left\lvert\frac{u_2(x_k)-u_{2,51}(x_k)}{u_2(x_k)}\right\rvert$
0.16	1.14655	1.14616	3.83251×10^{-4}	3.34266×10^{-4}
0.32	1.26380	1.26342	3.85271×10^{-4}	3.04851×10^{-4}
0.48	1.34877	1.34839	3.83138×10^{-4}	2.84064×10^{-4}
0.64	1.39929	1.39892	3.75127×10^{-4}	2.68084×10^{-4}
0.80	1.41406	1.41370	3.59590×10^{-4}	2.54296×10^{-4}
0.96	1.39271	1.39238	3.35005×10^{-4}	2.40542×10^{-4}

Example 2 *Consider the following SFIDEs*

$$\begin{cases} {}_0^{ABC}\mathfrak{D}_x^{\alpha} u_1(x) = \frac{1}{\Gamma(\alpha)} \int_0^x (x-\tau)^{\alpha-1} u_2(\tau) d\tau + \frac{5}{4}(1+x), \\ {}_0^{ABC}\mathfrak{D}_x^{\alpha} u_2(x) = \frac{1}{\Gamma(\alpha)} \int_0^x (x-\tau)^{\alpha-1} u_1(\tau) d\tau + \frac{7}{4}(1+x), \end{cases}$$

with the nonlocal boundary conditions:

$$\begin{cases} u_1(0) + \frac{2}{5} u_1(1) - \sin(1.352) \int_0^1 u_1(x) dx = 0, \\ u_2(0) + \frac{2}{3} u_2(1) - \tan(1.004) \int_0^1 u_2(x) dx = 0, \end{cases}$$

Table 3: Numerical outcomes for the approximate solution $u_{1.21}(x)$ at different values of α for Example (1).

x_k	α=1	α=0.95	α=0.85	α=0.75
0.1	0.895216	0.763427	0.862165	0.663817
0.2	0.781462	0.653123	0.749839	0.555434
0.3	0.659898	0.538629	0.630672	0.445503
0.4	0.531736	0.420308	0.505833	0.333497
0.5	0.398256	0.299119	0.376522	0.220117
0.6	0.260788	0.176139	0.243991	0.106245
0.7	0.120703	0.052457	0.109522	-0.00723
0.8	-0.020601	-0.070842	-0.025587	-0.11945
0.9	-0.161717	-0.192690	-0.160039	-0.22958

Table 4: Numerical outcomes for the approximate solution $u_{2,21}(x)$ at different values of α for Example (1).

x_k	α=1	α=0.95	α=0.85	α=0.75
0.1	1.092630	1.197960	1.118240	1.278340
0.2	1.176520	1.252500	1.192200	1.313070
0.3	1.248630	1.294380	1.254450	1.333880
0.4	1.308260	1.323770	1.304340	1.341890
0.5	1.354800	1.340410	1.341360	1.337150
0.6	1.387790	1.344070	1.365120	1.319720
0.7	1.406920	1.334710	1.375400	1.289760
0.8	1.411980	1.312410	1.372110	1.247660
0.9	1.402940	1.277460	1.355290	1.193920

Table 5: Numerical outcomes for the solution $u_1(x)$ of Example (2) at $\alpha = 1$.

x_k	$u_1(x_k)$	$u_{1,51}(x_k)$	$\lvert u_1(x_k) - u_{1,51}(x_k)\rvert$	$\frac{\lvert u_1(x_k) - u_{1,51}(x_k)\rvert}{\lvert u_1(x_k)\rvert}$
0.16	0.217244	0.217246	2.63589×10^{-6}	1.21334×10^{-5}
0.32	0.474359	0.474372	1.35885×10^{-5}	2.86460×10^{-5}
0.48	0.780416	0.780442	2.66698×10^{-5}	3.41738×10^{-5}
0.64	1.145950	1.145990	4.23195×10^{-5}	3.69298×10^{-5}
0.80	1.583150	1.583210	6.10411×10^{-5}	3.85568×10^{-5}
0.96	2.106130	2.106210	8.34128×10^{-5}	3.96048×10^{-5}

where $0 \leq \alpha \leq 1$. *The exact solution at* $\alpha = 1$ *is*

$$\begin{cases} u_1(x) = -(0.75 + 1) + \frac{3\exp(x)}{2} - \frac{1}{2}(1 - 20.75)(\cos(x) - \sin(x)), \\ u_2(x) = (0.75 - 2) + \frac{3\exp(x)}{2} + \frac{1}{2}(1 - 20.75)(\cos(x) - \sin(x)). \end{cases}$$

Indeed, the exact solution at the fractional value of α *is not available.*

By applying the proposed method to solve Example (2). We display the numerically representative results in Tables 5–8. Error analysis at some selected grid points with step size $h = 0.16$ *and* $n = 51$ *when* $\alpha = 1$ *are summarized in Tables 1 and 2. Furthermore, using the present method, we pick uniform grid points* $x_k = \frac{k-1}{n-1}$, $i = 1, 2, \ldots, n$. *The numerical outcomes for different values of the fractional-order* α *are given in Tables 3 and 4 to explain the approximate solutions such that* $\alpha \in \{0.75, 0.85, 0.95, 1\}$ *and* $n = 11$. *Also, in Figures 1 and 2, we represent the numerical data graphically in the form of graphic curves in order to study the behavior of approximate solutions at different values for* α *and study the error analysis compared with the exact solution at* $\alpha = 1$.

Here, it is obvious that numerical solutions are in close coincidence with each other.

6 Conclusion

In this work, we apply a flexible and precise iterative numerical approach, reproducing kernel discretization method (RKDM), in order to explore solutions of SFIDEs subject to the integral boundary conditions

Table 6: Numerical outcomes for the solution $u_2(x)$ of Example (2) at $\alpha = 1$.

x_k	$u_2(x_k)$	$u_{2,51}(x_k)$	$\lvert u_2(x_k) - u_{2,51}(x_k)\rvert$	$\frac{\lvert u_2(x_k) - u_{2,51}(x_k)\rvert}{\lvert u_2(x_k)\rvert}$
0.16	0.30328	0.30329	1.87581×10^{-6}	6.18492×10^{-6}
0.32	0.65702	0.65703	9.81961×10^{-6}	1.49456×10^{-5}
0.48	1.06781	1.06783	1.96850×10^{-5}	1.84350×10^{-5}
0.64	1.54350	1.54353	3.20966×10^{-5}	2.07947×10^{-5}
0.80	2.09347	2.09352	4.77527×10^{-5}	2.28103×10^{-5}
0.96	2.72896	2.72903	6.74244×10^{-5}	2.47070×10^{-5}

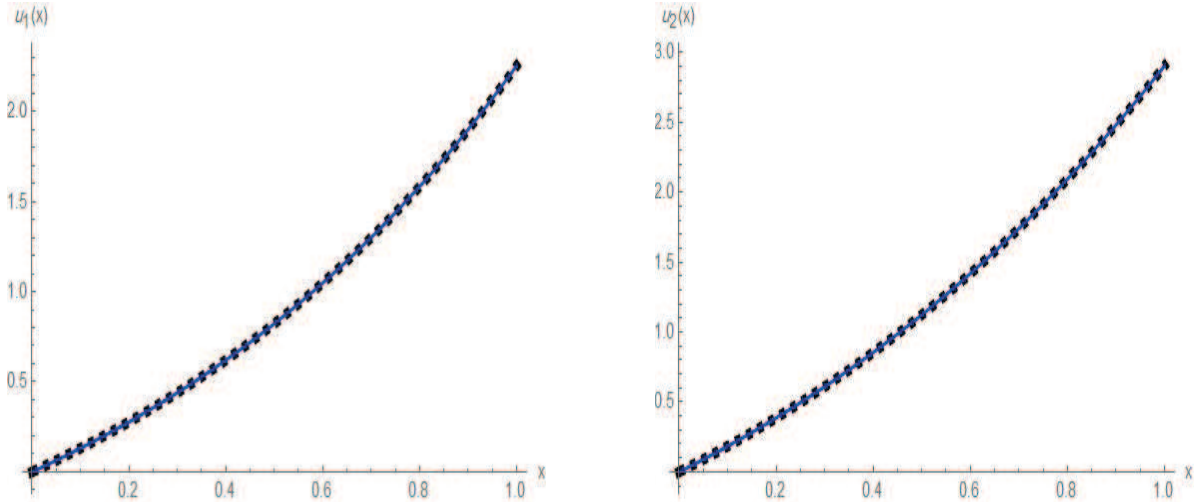

(a) (b)

Figure 1: Comparison of the exact solution and the approximate solutions (with $n = 51$) for Example (2) with $\alpha = 1$.

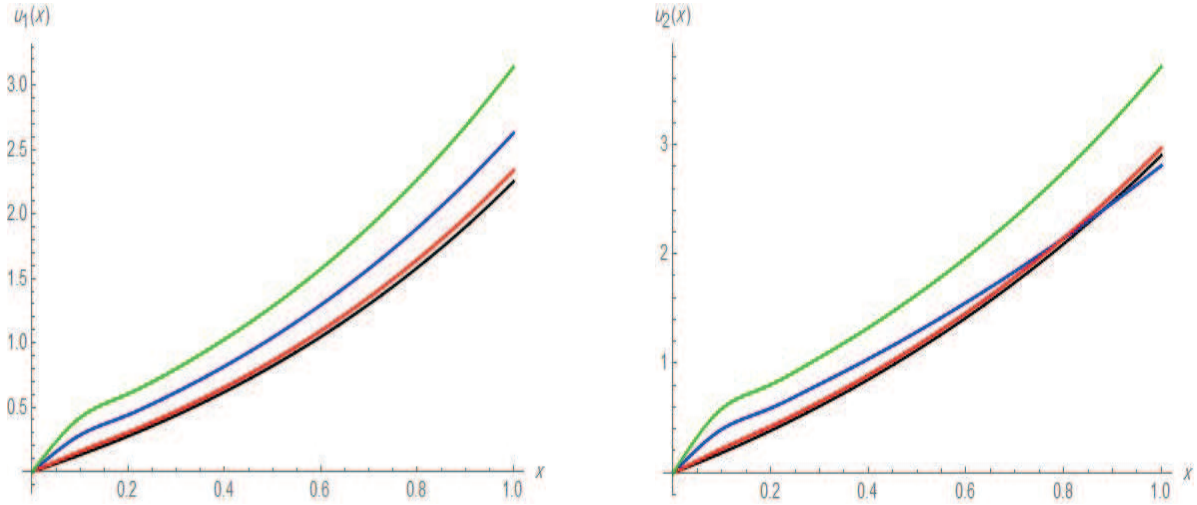

(a) (b)

Figure 2: The behavior of approximate solutions at different values of Example (2) for $n = 11$ at different values of α: "Black" $\alpha = 1$,"Blue" $\alpha = 0.95$,"Red" $\alpha = 0.85$, and "Green" $\alpha = 0.75$.

Table 7: Numerical outcomes for the approximate solution $u_{1,11}(x)$ at different values of α for Example (2).

x_k	α=1	α=0.95	α=0.85	α=0.75
0.1	0.131264	0.284930	0.157123	0.420116
0.2	0.277012	0.441727	0.305443	0.605207
0.3	0.439425	0.619162	0.470347	0.800601
0.4	0.620469	0.818675	0.654918	1.028600
0.5	0.822598	1.043230	0.861889	1.284820
0.6	1.048500	1.295180	1.093940	1.574880
0.7	1.301120	1.576950	1.354070	1.901450
0.8	1.583690	1.891440	1.645740	2.268900
0.9	1.899730	2.240780	1.971940	2.680540

Table 8: Numerical outcomes for the approximate solution $u_{2,11}(x)$ at different values of α for Example (2).

x_k	α=1	α=0.95	α=0.85	α=0.75
0.1	0.183760	0.398323	0.220059	0.586464
0.2	0.386437	0.590778	0.424416	0.805510
0.3	0.609601	0.810051	0.648416	1.053710
0.4	0.854689	1.040980	0.894579	1.326370
0.5	1.123510	1.290500	1.165180	1.630350
0.6	1.418100	1.557010	1.462230	1.966760
0.7	1.740700	1.841510	1.788120	2.339430
0.8	2.093850	2.144510	2.145660	2.752070
0.9	2.480380	2.466290	2.537270	3.207920

emerging in the framework of Atangana-Baleanu fractional concepts. This approach is mainly based on the reproducing kernel theory which has widely used applications. The obtained results show the accuracy and effectiveness of the RKDM on dealing with such types of systems emerging in the Atangana-Baleanu frameworks.

References

[1] K. S. Miller and B. Ross, An Introduction to the Fractional Calculus and Fractional Differential Equations, John Willy and Sons, New York, 1993.

[2] R. Hilfer, Application of Fractional Calculus in Physics, World Scientific, 2000.

[3] I. Podlubny, Fractional Differential Equations, Academic Press, San Diego, 1999.

[4] M. Al-Smadi, Fractional residual series for conformable time-fractional Sawada-Kotera-Ito, Lax, and Kaup-Kupershmidt equations of seventh order, Math. Meth. Appl. Sci., (2021), 1–22.

[5] M. Al-Smadi, O. A. Arqub and D. Zeidan, Fuzzy fractional differential equations under the Mittag-Leffler kernel differential operator of the ABC approach: theorems and applications, Chaos, Solitons and Fractals, 146(2021), 14 pp.

[6] M. Fardi, S. Al-Omari and S. Araci, A pseudo-spectral method based on reproducing kernel for solving the time-fractional diffusion-wave equation, Advan. Continuous Disc. Models, 1(2022), 1–14.

[7] M. Heydari, E. Shivanian, B. Azarnavid and S. Abbasbandy, An iterative multistep kernel based method for nonlinear Volterra integral and integro-differential equations of fractional order, J. Comput. Appl. Math., 361(2019), 97–112.

[8] X. C. Zhong, X. L. Liu and S. L. Liao, On a generalized Bagley-Torvik equation with a fractional integral boundary condition, Int. J. Appl. Comput. Math., 3(2017), 727–746.

[9] M. Shqair, M. Alabedalhad, S. Al-Omari and M. Al-Smadi, Abundant exact travelling wave solutions for a fractional massive Thirring model using extended Jacobi elliptic function method, Fractal Fract., 252(2022), 1–16.

[10] F. Mainardi, Fractional Calculus and Waves in Linear Viscoelasticity: An Introduction to Mathematical Models, Imperial College Press, 2015.

[11] A. Atangana and D. Baleanu, New fractional derivatives with nonlocal and non-singular kernel: Theory and application to heat transfer model, Thermal Science, 20(2016), 763–769.

[12] M. Al-Smadi, H. Dutta, S. Hasan and S. Momani, On numerical approximation of Atangana-Baleanu-Caputo fractional integro-differential equations under uncertainty in Hilbert Space, Math. Model. Nat. Phenom., 16(2021), 41.

[13] S. Zaremba, L'equation biharmonique et une classe remarquable de fonctions fondamentales harmoniques, Imprimerie de l'Universite, 1907.

[14] F. Geng and M. Cui, New method based on the HPM and RKHSM for solving forced Duffing equations with integral boundary conditions, J. Comput. Appl. Math., 233(2009), 165–172.

[15] C. L. Li and M. G. Cui, The exact solution for solving a class of nonlinear operator equations in the reproducing kernel space, Appl. Math. Comput., 143(2003), 393–399.

[16] S. Hasan, N. Djeddi, M. Al-Smadi, S. Al-Omari, S. Momani and A. Fulga, Numerical solvability of generalized Bagley-Torvik fractional models under Caputo-Fabrizio derivative, Adv. Difference Equ., 469(2021), 21 pp.

[17] M. Cui and Y. Lin, Nonlinear Numerical Analysis in The Reproducing Kernel Space, Nova Science Publishers, Inc., New York, 2009.

[18] M. Al-Smadi, O. A. Arqub, N. Shawagfeh and S. Momani, Numerical investigations for systems of second-order periodic boundary value problems using reproducing kernel method, Appl. Math. Comput., 291(2016), 137–148.

[19] S. Momani, N. Djeddi, M. Al-Smadi and S. Al-Omari, Numerical investigation for Caputo-Fabrizio fractional Riccati and Bernoulli equations using iterative reproducing kernel method, Appl. Numer. Math., 170(2021), 418–434.

[20] S. Hasan, A. El-Ajou, S. Hadid, M. Al-Smadi and S. Momani, Atangana-Baleanu fractional framework of reproducing kernel technique in solving fractional population dynamics system, Chaos Solitons Fractals, 133(2020), 10 pp.

[21] N. Djeddi, S. Hasan, M. Al-Smadi and S. Momani, Modified analytical approach for generalized quadratic and cubic logistic models with Caputo-Fabrizio Fractional derivative, Alexandria Engineering Journal, 59(2020), 5111–5122.

[22] M. Al-Smadi, O. Abu Arqub and M. Gaith, Numerical simulation of telegraph and Cattaneo fractional-type models using adaptive reproducing kernel framework, Math. Methods Appl. Sci., 44(2021), 8472–8489.

[23] N. Harrouche, S. Momani, S. Hasan and M. Al-Smadi, Computational algorithm for solving drug pharmacokinetic model under uncertainty with nonsingular kernel type Caputo-Fabrizio Fractional derivative, Alexandria Engineering Journal, 60(2021), 4347–4362.

[24] M. Alaroud, N. Tahat, O. Ababneh, S. Al-Omari, Analytic technique for solving temporal time-fractional gas dynamics equations with Caputo fractional derivative, AIMS Math., 7(2022), 17647–17669.

[25] M. Al-Smadi, N. Djeddi, S. Momani, S. Al-Omari and S. Araci, An attractive numerical algorithm for solving nonlinear Caputo-Fabrizio Fractional Abel differential equation in a Hilbert space, Adv. Difference Equ., (2021), 18 pp.

[26] M. Al-Smadi, Simplified iterative reproducing kernel method for handling time-fractional bvps with error estimation, Ain Shams Engineering Journal, 9(2018), 2517–2525.

[27] M. Al-Smadi and O. A. Arqub, Computational algorithm for solving Fredholm time-fractional partial integrodifferential equations of Dirichlet functions type with error estimates, Appl. Math. Comput., 342(2019), 280–294.

[28] M. Shqair, M. Alabedalhad, S. Al-Omari and M. Al-Smadi, Abundant exact travelling wave solutions for a fractional massive Thirring model using extended Jacobi elliptic function method, Fractal Fract, 6(2022), 1-16.

[29] G. Gumah, M. F. M. Naser, M. Al-Smadi, S. K. Q. Al-Omari and D. Baleanu, Numerical solutions of hybrid fuzzy differential equations in a Hilbert space, Appl. Numer. Math., 151(2020), 402–412.

[30] Y. Al-qudah, M. Alaroud, H. Qoqazeh, A. Jaradat, S. AlHazmi and S. Al-Omari, Approximate analytic-numeric fuzzy solutions of fuzzy fractional equations using residual power series approach, Symmetry 14(2022), 804, 1–19.

[31] Z. Altawallbeh, M. Al-Smadi, I. Komashynska and A. Ateiwi, Numerical solutions of fractional systems of two-point bvps by using the iterative reproducing kernel algorithm, Ukrainian Math. J, 70(2018), 687–701.

[32] M. Alaroud, N. Tahat, O. Ababneh and S. Al-Omari, Analytic technique for solving temporal time-fractional gas dynamics equations with Caputo fractional derivative, AIMS Math., 7(2022), 17647–17669.

[33] M. Alabedalhadi, M. Al-Smadi, S. Al-Omari and S. Momani, New optical soliton solutions for coupled resonant Davey-Stewartson system with conformable operator, Optical and Quantum Electronics, 54(2022), 1–20.